The mdx mouse is an animal model for human Duchenne dystrophy. In both disorders, the muscle fiber plasma membrane is rendered selectively vulnerable by dystrophin deficiency. In both disorders there are also ultrastructural abnormalities involving the postsynaptic membrane of the neuromuscular junction. The object of this electrophysiologic study was to determine whether the observed ultrastructural abnormalities at the mdx neuromuscular junction are associated with an abnormality of neuromuscular transmission. In comparison with age-matched control mice, the mdx mice show an abnormal, age-dependent decrease of the amplitude of the miniature end-plate potential and a concomitant increase in the quantal content of the end-plate potential. Consequently, the safety margin of neuromuscular transmission is not impaired.
Key words: mdx mouse • muscular dystrophy • neuromuscular transmission • neuromuscular junction • acetylcholine receptor

MUSCLE & NERVE 13:742–749 1990

NEUROMUSCULAR TRANSMISSION IN THE mdx MOUSE

ALEXANDRE NAGEL, MD, FRANK LEHMANN-HORN, MD, and ANDREW G. ENGEL, MD

The recent discovery of dystrophin deficiency in Duchenne dystrophy (DD) contributed importantly to understanding the pathogenesis of DD (reviewed in reference 17). Dystrophin is a cytoskeletal protein associated with the sarcolemma, and its deficiency provides a plausible explanation for sarcolemmal defects which develop early in the course of muscle fiber destruction in DD.[6,24]

It is also noteworthy that about half of the DD end-plates show ultrastructural abnormalities consisting of focal degeneration of the junctional folds, simplification of the postsynaptic region and/or widening of the synaptic cleft.[18] Another possible indicator of end-plate involvement in DD is an abnormal jitter detected in single fiber EMG.[15] The cause, significance, and consequences of involvement of the neuromuscular junction (NMJ) in DD have received little attention.

In vitro studies of neuromuscular transmission have been carried out in a small number of DD patients; the only abnormality detected has been a reduced resting membrane potential (RMP).[26] However, in view of the fact that dystrophin is now known to be concentrated in the postsynaptic region of the NMJ,[3] a more extensive study of neuromuscular transmission was appropriate. The mdx mouse,[2] an animal model of DD, was used. Several studies support the validity of the model: dystrophin is absent from mdx mouse muscles;[1,16,29,31] this deficiency is associated with sarcolemmal defects, fiber necrosis and regeneration. Further, the ultrastructural changes at the NMJ are similar to those noted in human DD (Mora M and Engel AG, 1986, unpublished observation, and reference 30). The object of this study was to further analyze the morphologic and physiologic aspects of the mdx NMJ.

METHODS

The Mayo Clinic's Animal Care and Use Committee's guidelines were followed in our experiments. The mdx mice were a gift from Dr. G. Bulfield (Poultry Research Centre, Roslin Midlothian, UK). Normal C57B/10 strain mice (Jackson Laboratories, Bar Harbor, ME) were used as controls. In a pilot study, we examined the pathologic alter-

From the Department of Neurology and Neuromuscular Research Laboratory, Mayo Clinic, Rochester, Minnesota (Drs. Nagel and Engel) and the Neurologische Klinik und Polyklinik der Technischen Universität München, West Germany (Dr. Lehmann-Horn).

Supported by NIH grant NS 6277, a Research Center Grant from the Muscular Dystrophy Association and the Mogg Fund. Dr. Nagel was the recipient of a postdoctoral research fellowship from the Muscular Dystrophy Association.

Address correspondence to Dr. Andrew Engel, Department of Neurology and Neuromuscular Research Laboratory, Mayo Clinic, Rochester, MN 55905.

Accepted for publication December 15, 1989.

CCC 0148–639X/90/080742–08 $04.00

ations in the diaphragms of 1 to 16 week old mdx mice. Fiber necrosis and regeneration were most active around 4 weeks of age. Because necrotic fibers are not suitable for electrophysiologic studies of the NMJ, mice were studied at 2½ weeks, before the onset of massive fiber necrosis, at 8½ weeks, by when the acute necrotizing phase has subsided, and at 37 weeks, when the disease has become chronic. For each age group, diaphragm muscles were obtained from 6 to 7 mdx and from 5 to 8 control mice. A total of 38 diaphragms were studied.

One part of each diaphragm was mounted in a bath continuously perfused with oxygenated (95% O_2 + 5% CO_2) Tyrode solution containing (m*M*): NaCl, 135; Na_2HPO_4, 1.3; $NaHCO_3$, 15; KCl, 5; $CaCl_2$, 2; $MgCl_2$, 1.0; glucose, 11.1; and pH 7.2.[5] For the study of end-plate potentials (EPP), 3.7 to 4.0 μM tubocurarine was added to prevent twitching. The RMP, miniature end-plate potentials (MEPP) and end-plate potentials (EPP) were recorded at 29 to 30°C with conventional intracellular microelectrodes with 8 to 12 M-ohm resistance connected to an Axoprobe 1A microelectrode amplifier and an A1 2130 differential amplifier (Axon Instruments, Inc., Burlingame, CA). The resulting signal was digitized at 20 kHz and then analyzed with an Indec Data Acquisition System (Indec Systems, Inc., Sunnyvale, CA). Fibers whose RMP dropped more than 10 mV during recording were excluded from the analysis. The analysis was restricted to focal recordings in which the MEPP and EPP rise times were less than 1 msec. MEPP and EPP amplitudes were corrected to a standard RMP of −80 mV assuming an equilibrium potential of 0 mV[19,22]; EPP amplitudes were also corrected for nonlinear summation.[23] MEPP with more than twice the mean amplitude were rejected as "giant MEPP." In each diaphragm, MEPP and EPP were recorded from at least 10 different fibers. For MEPP recordings, 50 potentials were collected in each fiber. For EPP recordings, the phrenic nerve was stimulated with a suction electrode with a train of 100 stimuli at 0.5 Hz. The second 50 EPP in each train were used to calculate the quantal content, *m*, according to the formula:[21]

$$m = (\text{mean EPP amplitude})^2/(\text{EPP variance} - \text{background noise variance})$$

The other part of each diaphragm was processed for conventional histochemical[7] and other morphologic studies. In cryostat sections of each diaphragm, the geometric mean of the shortest and longest caliper diameter[4] was determined in 50 randomly selected muscle fibers at a final magnification of 700×.

At the age of 37 weeks, strips from two mdx and two control diaphragms were processed for electron microscopy as described earlier.[25] Electron micrographs of end-plates were printed at a final magnification of 26,000×. The nerve terminal area, synaptic vesicle density, and the number of active zones per μm presynaptic membrane length were determined by previously described morphometric methods.[8,11] Other diaphragm strips were prepared for the ultrastructural localization of acetylcholine receptors (AChR) by modification of a previously described method.[10] In brief, fresh muscle strips were incubated with biotinylated alpha-bungarotoxin (6 μg/mL, Molecular Probes Inc., Eugene, OR). After rinsing, fixation and dissection of the end-plates, avidin and biotinylated horseradish peroxidase were added (ABC kit, Vector Laboratories, Burlingame, CA), and after a further rinse the reaction product was developed by the DAB method. Electron micrographs produced by this technique were used to determine the AChR index (length of postsynaptic membrane reacting for alpha-bungarotoxin/presynaptic membrane length).[8]

At each age, glutaraldehyde-fixed muscle strips were stained for acetylcholinesterase[13] in two mdx and two control mice; the maximal longitudinal length of about 25 to 50 NMJ was then measured in each strip. Other diaphragm strips containing at least 250 end-plates were used to estimate the number of NMJ-specific ^{125}I-alpha-bungarotoxin binding sites.[12]

RESULTS

Observations in Cryostat Sections. Pathologic changes were present in muscles of all mdx mice (Table 1). At 2½ weeks, all but one of the animals showed fiber necrosis, and in all animals a small

Table 1. Summary of histologic abnormalities in *mdx* diaphragm muscles.*

Age	Necrotic fibers (%)	Nonnecrotic fibers with central nuclei (%)
2½ weeks	1–5	4
8½ weeks	10–30	60
37 weeks	5	60

**Values given represent estimates from 5 muscles at 2½ weeks and 6 muscles at 8½ and 37 weeks.*

percentage of fibers contained central nuclei. At 8½ weeks, the histologic changes in mdx muscles were more extensive: up to about one-third of the fibers were necrotic and central nuclei were found in more than half of the nonnecrotic fibers. At 37 weeks, the percentage of necrotic fibers was lower, but more than half of the nonnecrotic fibers had central nuclei. There was a mild to moderate increase of endomysial and perimysial connective tissue at 8½ and 37 weeks. Diaphragm muscles of control mice showed no fiber necrosis and none of the fibers had central nuclei at any age.

Changes in RMP, MEPP, and Fiber Diameter. The RMP showed no age dependence. When all control and mdx recordings were compared, the RMP was significantly reduced from 63.6 ± 0.9 (mean ± SEM) mV (n = 19) in control muscles to 60.3 ± 1.0 mV (n = 17) in mdx muscles (P < 0.025).

The frequency, rise time, and decay time constant of MEPPs in mdx animals did not differ significantly from the corresponding values in age-matched controls.

The MEPP amplitudes decreased with age in both groups. However, in mdx mice this decrease was more marked than in the controls (Fig. 1). The depression of the MEPP amplitudes in the mdx mice was not statistically significant at 2½ and 8½ weeks, but became statistically significant at 37 weeks when the mdx value was reduced by 26% (Table 2).

Because the MEPP amplitude is inversely proportional to the 3/2 power of the fiber diameter,[19] a decrease in MEPP amplitude in the mdx mice could have been secondary to an increase in fiber diameter. However, the mean fiber diameters in mdx and control mice were not significantly different at 2½ and 8½ weeks, and at 37 weeks, the mdx value was 23% smaller than the corresponding control value (Table 3). Hence, the reduction in MEPP amplitude in mdx mice could not be due to an increase in mean fiber diameter.

Table 2. Electrophysiologic findings.*

Experimental group	MEPP amplitude (mV)	Quantal content *(m)*
2½ weeks:		
Control	1.46 ± 0.09 (5)	56.9 ± 6.1 (5)
mdx	1.34 ± 0.15 (6)	64.5 ± 6.4 (4)
P†	NS	NS
8½ weeks:		
Control	1.19 ± 0.05 (6)	106.8 ± 7.4 (5)
mdx	1.00 ± 0.08 (6)	132.2 ± 5.3 (5)
P†	NS	<0.025
37 weeks:		
Control	1.21 ± 0.06 (8)	117.6 ± 4.7 (6)
mdx	0.90 ± 0.06 (7)	183.6 ± 12.7 (5)
P†	<0.005	<0.001

*Values given are mean ± SEM and number of animals (in parentheses).
†Student's two-tailed t-test.
NS = not significant.

Changes in Quantal Content and End-Plate Length. In contrast to the MEPP amplitudes, the quantal

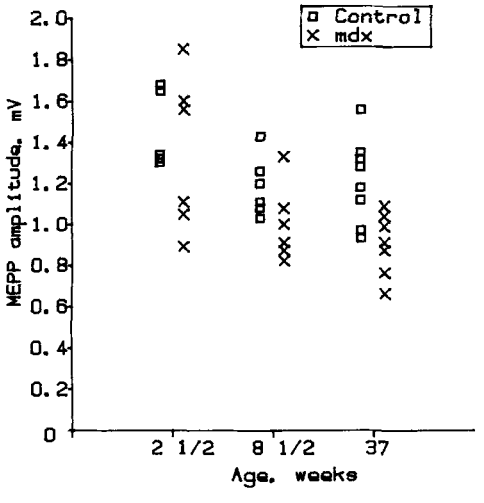

FIGURE 1. MEPP amplitudes in mdx and age-matched control mice. Each symbol represents the mean for one animal.

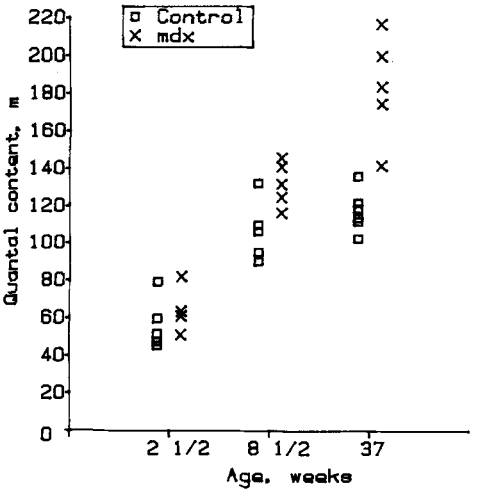

FIGURE 2. EPP quantal contents in mdx and age-matched control mice. Each symbol represents the mean for one animal.

Table 3. Muscle fiber diameter, end-plate size and AChR content.

Experimental group	Muscle fiber diameter (μm)*	End-plate length (μm)†	^{125}I-alpha bungarotoxin binding sites per end-plate (10^6)*
2½ weeks:			
Control	26.2 ± 1.1 (5)	24.2 ± 0.7 (75)	6.23 ± 0.59 (2)
mdx	26.3 ± 1.5 (5)	28.9 ± 0.9 (76)	7.74 ± 0.59 (2)
P‡	NS	<0.001	NS
8½ weeks:			
Control	35.4 ± 0.8 (6)	31.1 ± 0.9 (96)	11.31 ± 2.69 (2)
mdx	33.2 ± 1.6 (6)	33.1 ± 0.8 (93)	15.15 ± 2.40 (2)
P‡	NS	NS	NS
37 weeks:			
Control	37.2 ± 1.0 (6)	33.8 ± 1.1 (101)	21.78 ± 0.18 (2)
mdx	28.8 ± 1.5 (6)	40.7 ± 1.4 (101)	21.74 ± 0.64 (2)
P‡	<0.001	<0.001	NS

**Mean ± SE and number of animals (in parentheses).*
†Mean ± SE and number of end-plates analyzed (in parentheses).
‡Student's two-tailed t-test.
NS = not significant.

content of the EPP increased with age in both animal groups. This increase was greater in mdx than control mice (Fig. 2) and the difference, which was 24% at 8½ weeks and 56% at 37 weeks, was statistically significant (Table 2). The length of the acetylcholinesterase reacted end-plate regions was increased in mdx mice, and the increase was highly significant at 2½ and 37 weeks (Table 3).

^{125}I-Alpha-Bungarotoxin Binding. There was no significant difference in the total number of AChR per end-plate between age-matched mdx and control mice (Table 3).

Ultrastructural Observations at 37 Weeks. Simple inspection showed that some mdx nerve terminals were small in the imaged region, and some end-

FIGURE 3. End-plate region in control mouse diaphragm, 37 weeks. The nerve terminal lies in a deep postsynaptic gutter. The upper parts of the numerous junctional folds react for AChR (electron dense material). The estimated AChR index value was 2.58. Unstained section. Calibration bar = 1 μm.

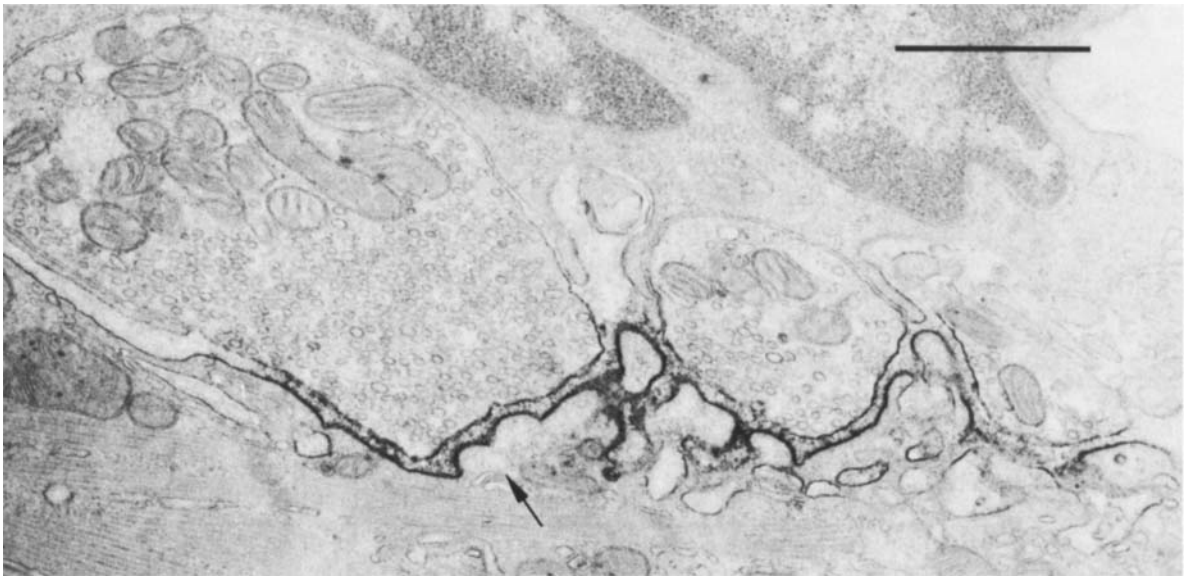

FIGURE 4. End-plate regions in mdx mouse diaphragm, 37 weeks. The two nerve terminals to the right are abnormally small. Junctional folds are absent or short (arrow) and the part of the postsynaptic membrane reacting for AChR is reduced; consequently, the AChR indices are reduced (1.08, 1.60, and 0.75 for the three terminals, from left to right). Also note the high density of synaptic vesicles. Unstained section. Calibration bar = 1 μm.

plates displayed postsynaptic simplification. These findings varied from end-plate to end-plate and from region to region within a given end-plate. A typical control end-plate region, which also shows the localization of AChR, is shown in Figure 3, and a typical mdx end-plate region can be seen in Figure 4. A more severely affected mdx end-plate with striking postsynaptic simplification is illustrated in Figure 5. Figure 6 illustrates a highly simplified mdx end-plate region. This region appears near degenerate material in the nearby basal lamina that probably represent remnants of preexisting junctional folds.

Morphometric Studies at 37 Weeks. The mean nerve terminal area was significantly reduced (Table 4), but the density of synaptic vesicles and the density of active zones at the presynaptic mem-

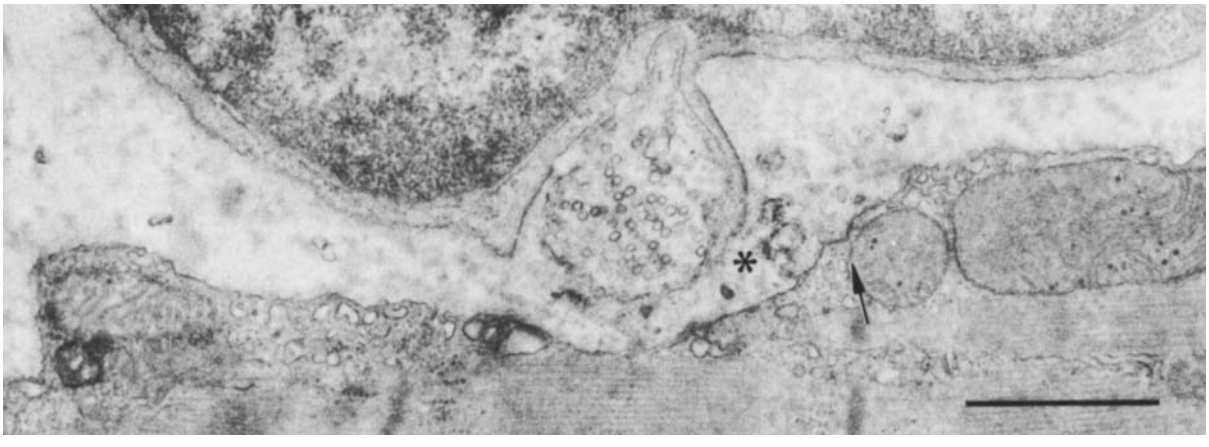

FIGURE 5. Degenerating NMJ in mdx mouse diaphragm, 37 weeks. The nerve terminal is small, the primary synaptic cleft is widened and contains electron dense material (asterisk). Secondary synaptic clefts are completely absent. There is only a minute portion of the postsynaptic membrane reacting for AChR (arrow). Unstained section. Calibration bar = 1 μ.

Table 4. Quantitative electronmicroscopy in 37 week-old mice.

Experimental group	Nerve terminal area (μm^2)*	Synaptic vesicle density (No./μm^2)†	Active zones (per μm)‡	AChR index§
Control	7.91 ± 0.83 (103)	57.5 ± 4.5 (10)	0.68 ± 0.07 (10)	2.66 ± 0.21 (23)
mdx	4.12 ± 0.46 (69)	76.5 ± 15.0 (10)	0.83 ± 0.08 (7)	1.80 ± 0.23 (19)
P#	<0.001	NS	NS	<0.01

**A total of 35 control and 22 mdx NMJ were available for analysis. Values indicate mean ± SE and number of nerve terminals analyzed (in parentheses). More than one nerve terminal can be found at a single NMJ.*
†10 NMJ were selected randomly from the 35 control NMJ and 10 NMJ were selected randomly from the 22 mdx NMJ. Vesicle densities in nerve terminals of a given NMJ were averaged for that NMJ. Values indicate the mean ± SE of vesicle densities for all NMJ in each group and the number of NMJ analyzed (in parentheses).
‡The same 10 randomly selected NMJ used for determining the synaptic vesicle density were analyzed, but 3 of 10 mdx NMJ were technically unsatisfactory for identifying active zones. The no. of active zones per μm presynaptic membrane length of each nerve terminal was averaged for a given NMJ. Values indicate the mean ± SE of active zone density for all NMJ in each group and the number of NMJ analyzed (in parentheses).
§Seven control and 10 mdx NMJ were available for analysis. Values indicate mean ± SE of AChR indices and the number of regions analyzed (in parentheses). More than one region can be found at a single NMJ.
#Student's two-tailed t-test.
NS = not significant.

brane were increased at the mdx end-plates. However, the increases in vesicle density and active zone density were not statistically significant. The data on the nerve terminal area and synaptic vesicle density in the control mice were close to values previously obtained by other workers.[30]

The AChR indices in mdx nerve terminals were significantly reduced. This was due to skewing of the frequency distribution to the left (Fig. 7).

DISCUSSION

The slight depression of the RMP in the mdx animals is similar to that reported in human DD.[26] This depression could be caused by changes in plasmalemmal permeability for sodium or potassium, or by structural membrane defects.

In comparison with age-matched controls, the MEPP amplitude was significantly decreased and the quantal content of the EPP was significantly increased in mdx mice at 37 weeks of age. It is possible that in mdx muscles the larger fibers were preferentially impaled. However, only at 2½ weeks were the large fibers more frequent in mdx than control diaphragms. At 37 weeks, when the MEPP reduction was most pronounced, the mean mdx fiber diameter was significantly smaller than the mean control fiber diameter. Also, at this age, 91% of the control fibers but only 41% of the mdx fibers were larger than 30 μm. Therefore, the reduced MEPP amplitude in mdx mice is not likely to be the result of selective sampling from larger diameter fibers. A change in specific membrane resistance is also unlikely to account for the reduced MEPP amplitude because the decay time

FIGURE 6. End-plate region in mdx mouse diaphragm, 37 weeks. The junctional folds are absent. The postsynaptic area is reacting for AChR, but the AChR index is low (1.12). Note degenerate material in basal lamina (asterisk). Stained section. Calibration bar = 1 μ.

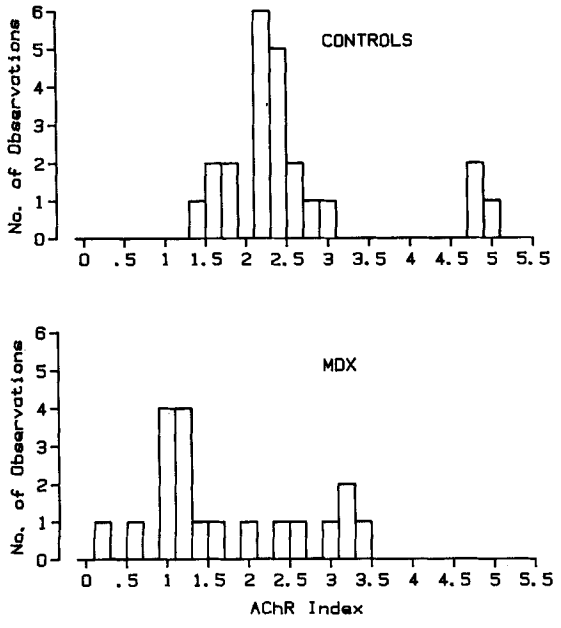

FIGURE 7. Frequency distribution of the AChR index in mouse diaphragm NMJ, 37 weeks. The mdx distribution is shifted to the left.

constant of the MEPP was not significantly different between the mdx mice and age-matched control mice.

The ultrastructural studies showed simplification of some postsynaptic regions and a significantly reduced mean AChR index for the mdx NMJ at 37 weeks. On the other hand, the number of ^{125}I-alpha-bungarotoxin binding sites in mdx mice was not significantly different from that in age-matched controls. However, the acetylcholinesterase stain showed that the mdx end-plates were significantly elongated at 37 weeks. This, in turn, implies that the AChR density per unit area of the mdx NMJ at 37 weeks was reduced, which is consistent with the ultrastructural data. The saturated disk model of neuromuscular transmission predicts that a reduced MEPP amplitude will result if the AChR density is reduced in individual end-plate regions[27] and, in fact, this is what was observed.

The increase in quantal content in mdx mice could be related to one or more of the following: (1) the overall enlargement of mdx end-plate area, (2) the increased synaptic vesicle density, and (3) the increased density of active zones on the presynaptic membrane. Although the increases in the last two parameters were not statistically significant, the combined increases provide a plausible explanation for the increase in quantal content. Under normal conditions, end-plate length is correlated positively with the muscle fiber diameter.[28] Because the mdx mice at 37 weeks had a reduced fiber diameter, the increase of their end-plate length is all the more significant.

The increased quantal content in mdx mice could be a compensatory reaction to offset the decreased MEPP amplitude and thereby maintain the safety margin of neuromuscular transmission. The safety margin (f) can be defined as:

$$f = (\text{MEPP amplitude} \times m) / (\text{RMP} - T)$$

where T is the threshold potential triggering the muscle fiber action potential.[14] Applying this formula under the assumption that T is unchanged in mdx mice, the safety margin in the mdx mice at 37 weeks was 1.5× higher (rather than smaller) than in the age-matched controls. A similar increase of end-plate size and safety margin has been described in the *dy* dystrophic mouse.[14,20]

It is likely that the alterations in neuromuscular transmission in mdx mice are conditioned by the dystrophin deficiency. The muscle membrane near the NMJ is subject to high mechanical stress and would therefore require abundant local expression of dystrophin.[3] Lack of dystrophin here could lead to mechanical injury of the junctinoal folds, with formation of small membrane defects on or near the folds. Calcium could then leak into the sarcoplasm and trigger focal degeneration of the junctional folds.[6] Shedding of injured segments of the folds into the synaptic space could contribute to the known appearance of the dystrophic endplates with postsynaptic simplification and debris in the synaptic cleft.[6] Focal degeneration of the junctional folds or simplification of the postsynaptic region will result in a decrease of AChR.[9] This adequately accounts for the observed alterations in the MEPP in the mdx mice.

REFERENCES

1. Bonilla E, Samitt CE, Miranda AF, et al: Duchenne muscular dystrophy: Deficiency of dystrophin at the muscle cell surface. *Cell* 1988;54:447–452.

2. Bulfield G, Siller WG, Wight PAL, Moore KJ: X chromosome-linked muscular dystrophy (mdx) in the mouse. *Proc Natl Acad Sci USA* 1984;81:1189–1192.

3. Chang HW, Bock E, Bonilla E: Dystrophin in electric organ of *Torpedo californica* homologous to that in human muscle. *J Biol Chem.* 1989;264:20831-20834.
4. Clancy MJ, Herlihy PD: Assessment of changes in myofibre size in muscle, in De Beer H, Martin J (Eds): *Central European Community Seminar on Patterns of Growth and Development in Cattle.* The Hague, Nyhoff, 1978, pp 203–218
5. Elmqvist D, Quastel DMJ: A quantitative study of end-plate potentials in isolated human muscle. *J Physiol (Lond.)* 1965;178:505–529.
6. Engel AG: Duchenne dystrophy, in Engel AG, Banker BQ (Eds): *Myology,* NY, McGraw-Hill, 1986, pp 1185-1240.
7. Engel AG: The muscle biopsy, in Engel AG, Banker BQ (Eds): *Myology,* New York, McGraw-Hill, 1986, pp 833–843.
8. Engel AG: Quantitative morphological studies of muscle, in Engel AG, Banker BQ (Eds): *Myology,* New York, McGraw-Hill, 1986, pp 1065–1072.
9. Engel AG, Banker BQ: Ultrastructural changes in diseased muscle, in Engel AG, Banker BQ (Eds): *Myology,* New York, McGraw-Hill, 1986, pp 909–1043.
10. Engel AG, Lindstrom JM, Lambert EH, Lennon VA: Ultrastructural localization of the acetylcholine receptor in myasthenia gravis and in its experimental autoimmune model. *Neurology* 1977;27:307–315.
11. Fukuoka T, Engel AG, Lang B, Newsom-Davis J, Vincent A: Lambert-Eaton myasthenic syndrome: II Immunoelectron microscopy localization of IgG at the mouse motor end-plate. *Ann Neurol* 1987;22:200–211.
12. Fumagalli G, Engel AG, Lindstrom J: Estimation of degradation rate of acetylcholine receptors by external gamma counting in vivo. *Mayo Clin Proc* 1982;57:758–764.
13. Gautron J: Cytochimie ultrastructurale des acétylcholinestérases. *Microscopie* 1974;21:259–264.
14. Harris JB, Ribchester RR: The relationship between end-plate size and transmitter release in normal and dystrophic muscles of the mouse. *J Physiol (Lond.)* 1979;296:245–265.
15. Hilton-Brown P, Stahlberg E: The motor unit in muscular dystrophy: A single fibre EMG and scanning EMG study. *J Neurol Neurosurg Psychiatry* 1983;46:981.
16. Hoffman EP, Brown RH, Kunkel LM: Dystrophin: The protein product of the Duchenne muscular dystrophy locus. *Cell* 1987;51:919–928.
17. Hoffman EP, Kunkel LM: Dystrophin abnormalities in Duchenne/Becker muscular dystrophy. *Neuron* 1989; 2:1019–1029.
18. Jerusalem F, Engel AG, Gomez MR: Duchenne dystrophy: II. Morphometric study of motor end-plate fine structure. *Brain* 1974;97:123–130.
19. Katz B, Thesleff S: On the factors which determine the amplitude of the 'miniature end-plate potential.' *J Physiol (Lond.)* 1957;137:267–278.
20. Kelly SS, Morgan GP, Smith JW: The origin of (+)-tubocurarine resistance in dystrophic mice. *Br J Pharmac* 1986;89:47–53.
21. Lang B, Newsom-Davies J, Prior C, Wray D: Antibodies to motor nerve terminals: an electrophysiological study of a human myasthenic syndrome transferred to mouse. *J Physiol (Lond.)* 1983;344:335–345.
22. Linder TM, Quastel DMJ: A voltage-clamp study of the permeability change induced by quanta of transmitter at the mouse end-plate. *J Physiol (Lond.)* 1978;281:535–558.
23. Martin AR: Quantal nature of synaptic transmission. *Physiol Rev* 1966;46:51–66.
24. Mokri B, Engel AG: Duchenne dystrophy: Electron microscopic findings pointing to a basic or early abnormality in the plasma membrane of the muscle fiber. *Neurology* 1975;25:1111–1120.
25. Mora M, Lambert EH, Engel AG: Synaptic vesicle abnormality in familial infantile myasthenia. *Neurology* 1987; 37:206–214.
26. Sakakibara H, Engel AG, Lambert EH: Duchenne dystrophy: Ultrastructural localization of the acetylcholine receptor and intracellular microelectrode studies of neuromuscular transmission. *Neurology* 1977; 27:741–745.
27. Salpeter MM: Vertebrate neuromuscular junctions: general morphology, molecular organization, and functional consequences, in Salpeter MM (Ed): *The vertebrate neuromuscular junction,* New York, AR Liss, 1987, pp 35–43.
28. Steinbach JH: Development changes in acetylcholine receptor aggregates at rat skeletal neuromuscular junctions. *Develop Biol* 1981;84:267–276.
29. Sugita H, Arahata K, Ishiguro T, Subara Y, Tsukahara T, Ishiura S, Eguchi C, Nonaka I, Ozawa E: Negative immunostaining of Duchenne muscular dystrophy (DMD) and mdx muscle surface membrane with antibody against synthetic peptide fragments predicted from DMD cDNA. *Proc Japan Acad* 1988;64(B):37–39.
30. Torres LFB, Duchen LW: The mutant mdx: inherited myopathy in the mouse. *Brain* 1987;110:269–299.
31. Voit T, Petel K, Dunn MJ, Dubowitz V, Strong PN: Distribution of dystrophin, nebulin and Ricinus communis I (RCA I)-binding glycoprotein in tissues of normal and mdx mice. *J Neurol Sci* 1989;89:199–211.